JOURNAL OF STRUCTURAL BIOLOGY **121,** 41–52 (1998)
ARTICLE NO. SB983964

Three-Dimensional Structure of HIV-1 Rev Protein Filaments

Norman R. Watts,* Manoj Misra,*,[1] Paul T. Wingfield,† Stephen J. Stahl,† Naiqian Cheng,* Benes L. Trus,*,‡ and Alasdair C. Steven*,[2]

Laboratory of Structural Biology Research, †Protein Expression Laboratory, National Institute of Arthritis and Musculoskeletal and Skin Diseases, and ‡Computational Bioscience and Engineering Laboratory, Division of Computer Research and Technology, and National Institutes of Health, Bethesda, Maryland 20892

Robert W. Williams§

§Department of Biochemistry, Uniformed Services University, 4301 Jones Bridge Road, Bethesda Maryland 20814

Received January 13, 1998

The HIV-1 Rev protein facilitates the export of incompletely spliced and unspliced viral mRNAs from the nucleus. Rev polymerizes into two types of filaments *in vitro*. In the presence of RNA, Rev forms poorly ordered structures, while in the absence of RNA it polymerizes into regular hollow filaments. We have determined the helical structure of the latter filaments by analysis of cryo-electron micrographs, taking into account STEM measurements of mass-per-unit-length. They are made up of Rev dimers, arranged in a six-start helix, with 31 dimers in 2 turns, a pitch angle of 45°, and an interstrand spacing of 3.8 nm. Three-dimensional reconstruction at 2.1 nm resolution reveals a smooth outer surface and a featured inner surface, with outer and inner diameters of ~14.8 and ~10.4 nm, respectively. The Rev dimer has a "top-hat" shape with a cylinder ~3.2 nm in diameter and ~2.2 nm high, pointing inward: the thinner rim areas pack together to form the filament wall. Raman spectroscopy shows polymerized Rev to have ~54% α-helix and 20–24% β-sheet content. Electron microdiffraction of aligned filaments reveals a broad meridional reflection at ~$(0.51\ nm)^{-1}$, suggesting approximate alignment of the α-helices with the filament axis. Based on these data, a molecular model for the Rev filament is proposed.

Key Words: **AIDS; cryo-electron microscopy; helical filaments; HIV-1; image reconstruction; Rev.**

INTRODUCTION

Human immunodeficiency virus (HIV-1) is the causative agent of acquired immune deficiency syndrome (AIDS). Regulation of viral replication involves two key transactivator proteins, Tat and Rev. Tat is an activator of transcription and, to a lesser extent, of translation. Rev, on the other hand, primarily enables the nucleocytoplasmic export of unspliced and partially spliced mRNAs, thus regulating the switch to the synthesis of structural proteins required in the late phase of the viral replication cycle (for reviews, see Cullen, 1992; Levy, 1993; Antoni *et al.*, 1994; Rosen and Fenyoe, 1995).

Rev is a small (13 kDa), basic (p*I* 9.2) protein with a high affinity for RNA (Heaphy *et al.*, 1991; Wingfield *et al.*, 1991; Daly *et al.*, 1993; Zemmel *et al.*, 1996). While Rev was originally thought to prevent or inhibit RNA splicing, either by disassembly of the spliceosome (Kjems *et al.*, 1993) or by coating the RNA (Wingfield *et al.*, 1991; Heaphy *et al.*, 1991), it is now thought to function largely by targeting the bound mRNA to an alternate export pathway, namely that normally used for 5S rRNA and snRNAs (Fisher *et al.*, 1995). Support for this proposal includes the observation that while all Rev-dependent mRNAs contain a Rev response element (RRE: Battiste *et al.*, 1996) they need not contain splice sites (Fisher *et al.*, 1994) and evidence that Rev interacts with a growing number of nucleoporin-like proteins (Fritz and Green, 1996; Bogerd *et al.*, 1995; Stutz *et al.*, 1995) and other cellular factors (Bevec *et al.*, 1996). Moreover, Rev has been shown to have both a nuclear export signal (NES) and a nuclear localization signal (NLS) and consequently to function as a nucleocytoplasmic shuttle protein that conveys transcripts to and through the nuclear pore (Görlich and Mattaj, 1996; Fritz and Green, 1996; Gerace, 1995). Rev may

[1] Present address: Unilever Research, 45 River Road, Edgewater, NJ 07020.

[2] To whom correspondence should be addressed at Bldg. 6, Room B2-34, 6 Center Drive MSC 2717, National Institutes of Health, Bethesda, MD 20892-2717. Fax: (301) 480-7629. E-mail: steven@calvin.niams.nih.gov.

1047-8477/98 $25.00

then escort mRNAs further into the cytoplasm to promote polysome association (Arrigo and Chen, 1991; Lawrence *et al.*, 1991), before returning to the nucleus for subsequent rounds of export, although this role in translation is probably secondary to that of facilitating mRNA export (Kingsman and Kingsman, 1996).

In vitro Rev readily forms polymers with two distinct morphologies. In the presence of RNA, whether cognate or heterologous, Rev rapidly forms poorly ordered filaments about 8 nm in diameter and of a length approximately proportional to the size of the RNA (Heaphy *et al.*, 1991; Wingfield *et al.*, 1991). These structures may be related to the complex which targets transcripts to the nuclear pore. In the absence of RNA and above the critical concentration of ~80 μg ml^{-1}, Rev assembles into regular, unbranched, filaments of indeterminate length, with an outer diameter of about 15 nm and an axial channel of 5–7 nm diameter, according to negative staining (Heaphy *et al.*, 1991; Wingfield *et al.*, 1991). Filament formation is an isodesmic process, driven primarily by a large negative enthalpy (Cole *et al.*, 1993).

It is this strong tendency to polymerize, as well as a general proclivity for aggregation and precipitation, that has so far thwarted attempts to solve the structure of Rev either by X-ray crystallography or by NMR spectroscopy. The only direct physical structure determination has been of a complex of a 22-amino-acid synthetic polypeptide, corresponding to the RNA binding helix of Rev (residues 33–55), bound to the minimal Rev-responsive element. Structural knowledge of Rev based on NMR (Battiste *et al.*, 1996), *in vivo* selection of variants of Rev (Jain and Belasco, 1996), circular dichroism and sequence considerations (Auer *et al.*, 1994), and functional analysis of targeted mutants (Thomas *et al.*, 1997) is therefore limited to a putative helix-turn-helix motif in the amino-terminal half of the protein (see Fig. 1).

In the absence of a monodisperse form of the intact protein at suitable concentrations, we have exploited the inherent order in the filaments to obtain structural information about Rev and the assemblies that it forms. Our initial strategy was to use electron microscopy to determine the helical geometry of subunit packing and fiber diffraction methods to record higher resolution data. Here we describe the structure of Rev filaments formed in the absence of RNA at 2.1 nm resolution as determined by cryo-electron microscopy and image reconstruction. Although X-ray fiber diffraction has not yet been fruitful, our EM data combined with conformational analysis by Raman spectroscopy and other, earlier observations allow us to propose a low-resolution model for the Rev dimer.

MATERIALS AND METHODS

Preparation of filaments. The overexpression and purification of Rev protein have been described in detail (Wingfield *et al.*, 1991). For this study Rev was unfolded in 6 M urea, diluted to 0.5 mg ml^{-1}, and refolded by sequential dialysis: first against 50 mM sodium phosphate, 600 mM ammonium sulfate, 150 mM sodium chloride, 50 mM sodium citrate, 1 mM EDTA, pH 7.0 (PASSE); then against 50 mM sodium phosphate, 150 mM sodium chloride, 50 mM sodium citrate, 1 mM EDTA, pH 7.0 (PSSE); and finally against 20 mM Hepes, 100 mM sodium chloride, 50 mM sodium citrate, 1 mM EDTA, pH 7.0 (HSSE). Rev filaments were stored at 4°C. As required, filaments were concentrated either by ultrafiltration (Centriprep-30, Amicon, Beverly, MA) or by pelleting at 142,000*g* for 5 h in a 45 Ti fixed-angle rotor (Beckman, Palo Alto, CA) and resuspension in a minimal volume of HSSE. Protein concentrations, corrected for light scattering, were determined as described by Wingfield *et al.* (1991).

Filaments of uniform length were prepared by initiating polymerization at a protein concentration of 0.65 mg ml^{-1}. The filaments thus formed were then stabilized against depolymerization and repolymerization by crosslinking lysine residues with 0.75 mM bis[sulfosuccinimidyl]suberate (BS^3, Pierce, Rockford, IL). They were then fractionated according to size, i.e., length, by gel filtration on a 2.6 × 95-cm column of Sephacryl Superfine S-1000 (Pharmacia-Biotech, Piscataway, NJ). Chromatography, using 10-ml samples, was performed with HSSE contain-

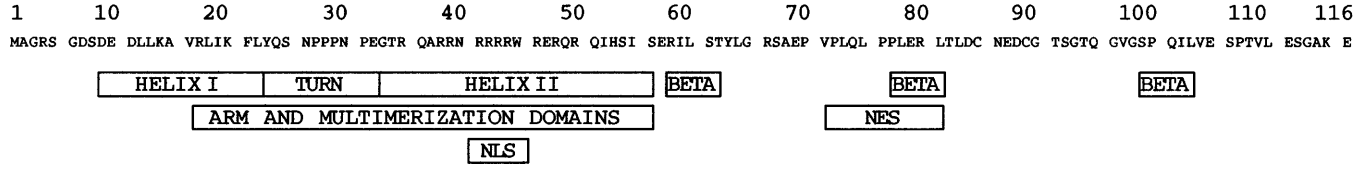

FIG. 1. Rev primary structure, key sequences, and domains. Shown are the predicted helix-turn-helix motif (Thomas *et al.*, 1997; Auer *et al.*, 1994); regions of predicted beta sheet (BETA; DSC secondary structure prediction); the arginine-rich motif (ARM) and the flanking (and possibly overlapping) "multimerization" domains; the nuclear localization signal (NLS) (Malim and Cullen, 1991; Zapp *et al.*, 1991); and the nuclear export signal (NES) (Fisher *et al.*, 1995).

ing 20 μg ml^{-1} protamine sulfate (Sigma, St. Louis, MO) at 4°C, with a flow rate of 0.4 ml min^{-1}. Filament length was monitored by electron microscopy (below). Prints of micrographs were scanned (Silverscanner II, LaCie, Beaverton, OR) and the filament lengths measured, using the program NIH Image (available at http://rsb.info.nih.gov/nih-image). The fraction of filaments selected for X-ray diffraction analysis had a length-to-width ratio (aspect ratio) of 17.6 ± 4.9 (SD, $n = 226$).

Alignment of Rev filaments. For X-ray fiber diffraction, specimens were prepared by the shearing method (Gregory and Holmes, 1965). Concentrated (100–150 mg ml^{-1}) solutions of Rev filaments with an aspect ratio of 18 (see above) were slowly drawn back and forth numerous times in the cold in 0.2-mm-diameter quartz capillaries (Charles Supper, Natick, MA) that had been treated with Sigmacote (Sigma). Most preparations were in HSSE, although the composition, ionic strength, and pH were also varied systematically. In some experiments, specimens were subsequently positioned for 12 to 24 h in the 8.5 Tesla magnetic field of a 360-MHz NMR magnet at 4°C in an attempt to improve the alignment (Torbet, 1987). X-ray diffraction was performed on a Rigaku X-ray set essentially as described by Wang and Stubbs (1994). Exposures ranged from 10 min to 6 h, and camera lengths between 90 and 75 mm were used. Capillaries were maintained at 4°C by a stream of nitrogen. Integrity of the liquid crystal was confirmed by polarizing microscopy before and after exposures.

Alignment on lipid monolayers. Monolayers were formed on slightly proud drops of PSSE buffer in 3.5-mm-diameter wells machined in a silicon block. Typically, lipid monolayers were formed by applying 5 μl of 1 mg ml^{-1} mixtures [1:8 to 1:1 (v/v)] of stearyl amine:egg yolk phosphatidyl choline (Avanti Polar Lipids Inc., Alabaster, AL) dissolved in chloroform onto 50 μl of buffer. After 30 min, 10 μl of 1 mg ml^{-1} Rev filaments was injected under the lipid monolayer. After ~4 h, arrays were picked up off the surface with carbon-coated grids, blotted, and stained with 2% phosphotungstic acid. Arrays were also prepared by several other methods. Arrays of 10–15 filaments were obtained by spreading solutions in 2% ammonium molybdate on freshly cleaved mica and, after drying and deposition of a thin covering layer of carbon, floating them off onto 2% uranyl acetate. Arrays were then scooped off the stain drop with 400 mesh carbon-coated copper grids (Ruiz *et al.*, 1994). Somewhat larger arrays could be formed by blotting the solutions unidirectionally across carbon-coated grids upon which 0.23-μm polystyrene beads had previously been deposited. The beads appeared to form channels that align the filaments. Small arrays were also formed by injecting urea-denatured Rev into buffer drops under lipid monolayers.

For electron diffraction studies, Rev filaments (60 mg ml^{-1} in PSSE) were aligned by smearing unidirectionally onto carbon-coated grids and then freezing immediately by plunging into liquid nitrogen-cooled liquid ethane.

Raman spectroscopy. Instrumentation and data analysis have been described previously (Williams, 1986). Solutions of Rev filaments at 100 mg ml^{-1} in PSSE were used. Raman amide I and amide III spectra were analyzed for secondary structure information using the nonnegative least-squares approach.

Structure prediction. Secondary structure prediction was determined using the DSC trained neural net (King and Sternberg, 1996). DSC may be accessed at http://bonsai.lif.icnet.uk/bmm/dsc/dsc_form_align.html.

Electron microscopy. Mass determinations of filaments were made from micrographs of freeze-dried specimens obtained at the Brookhaven STEM facility. Tobacco mosaic virus (TMV) included in the preparations served as a mass standard (Wall and Hainfeld, 1986; Thomas *et al.*, 1994).

For negative staining, Rev filaments at 0.1 mg ml^{-1} were adsorbed onto freshly air glow-discharged carbon-coated grids, rinsed with HSSE, and stained with 1% uranyl acetate. Micrographs were recorded with a Zeiss EM902 (Carl Zeiss, Thornwood, NY) at a nominal magnification of ×30 000. In some preparations, the filaments were rinsed with water, stained with methylamine vanadate (Nanoprobes, Stony Brook, NY), and examined in the STEM.

Electron microdiffraction (Kim *et al.*, 1996) of Rev was performed under low-dose conditions with a Philips EM 400 RT electron microscope, operating at 120 keV. The microscope was fitted with a blade-type liquid nitrogen-cooled anticontaminator. Diffraction patterns were recorded at a camera constant of 575 Åmm, while images, recorded after the diffraction pattern, were taken at ×2800 magnification on Kodak SO 163 film. Specimens consisted of Rev filaments smeared onto carbon-coated grids as described above. The electron-optical rotation between the image and the diffraction pattern was calibrated with unstained copper phthalocyanin crystals.

For cryo-electron microscopy, vitrified thin films of filaments suspended in HSSE on fenestrated carbon films were prepared by freezing in liquid ethane, essentially as described by Booy *et al.* (1991). Micrographs were recorded under low-dose conditions with a Philips CM20-FEG electron microscope (Philips, Eindhoven, Netherlands) equipped with a Gatan cryo-holder (Gatan, Pleasanton, CA) and operating

at 120 keV. Micrographs were recorded at a nominal magnification of ×38 000, subsequently calibrated relative to the 2.3-nm axial spacing of TMV particles included in the preparations. The micrographs were assessed for both defocus and stigmation by optical diffraction. For the micrographs employed here the first zero in the contrast transfer function (CTF) was at $(2.1\ \text{nm})^{-1}$.

Image processing. The analysis was performed essentially as described by Heck *et al.* (1996). Briefly, micrographs were digitized on a Perkin–Elmer 1010MG flatbed microdensitometer at a scanning rate of 0.52 nm per pixel. All processing was done with the PIC suite of programs (Trus *et al.*, 1996), running on an Alpha 3000-900 workstation (Digital Equipment Corp., MA). Filament images were computationally straightened (Steven *et al.*, 1986), whereupon the Fourier transforms and the corresponding diffraction patterns were calculated. From the relationship $J_n(2\pi R r_o) = \boldsymbol{X}_{max}$, where J_n is a Bessel function, R is the reciprocal radial distance, r_o is the mean radius of the particle, and $\boldsymbol{X}_{max}$ is the first maximum of the Bessel function, the most reasonable solution was 7.47, a value close to $\boldsymbol{X}_{max} = 7.5$ when $n = 6$, thus suggesting a six-start helix. An initial estimate of the number of subunits per turn was then determined from the mass-per-unit-length (70 kDa, as measured by STEM) and by constructing a helical surface lattice using spacings derived from the $(3.4\ \text{nm})^{-1}$ and $(5.3\ \text{nm})^{-1}$ layer lines in the diffraction pattern. Given the relative altitudes of these two layer lines, the integer selection rule $l = \pm 2n + 31m$, $n = 6n'$ was determined (see Results and Discussion). The images of the straightened particles were then scaled by interpolation in real space to bring all corresponding peaks on the layer lines to the same pixel row(s). The particles were then combined, i.e., scaled radially and brought into helical register by the appropriate angular and translational alignments. We attempted to assess the relative orientations of the particles—parallel or antiparallel—by comparing the minimized layer-line phase residual for both orientations, trying all pairwise combinations. However, no consistent polarities were found, either because the particles are nonpolar or because the polarity could not be detected at the current resolution. The contour level chosen for surface rendering of the density map corresponds to 120% of the volume of the calculated molecular mass using a partial specific volume of 0.712 $cm^3\ g^{-1}$ (Wingfield *et al.*, 1991). The cumulative filament length represented in the final reconstruction was 1.33 μm and corresponds to 7148 Rev monomers.

RESULTS AND DISCUSSION

Rev filaments: Control of aggregation and preparation of populations of uniform length. A major obstacle to working with Rev has been its tendency to aggregate and precipitate (Thomas *et al.*, 1997; Wingfield *et al.*, 1991, Heaphy *et al.*, 1991, Karn *et al.*, 1991). Aggregation involves at least two phenomena—polymerization of Rev into filaments and subsequent interactions between filaments (Fig. 2A). The most troublesome such interaction—side-to-side association—is at least partly temperature-dependent: Rev is more soluble in the cold (Wingfield *et al.*, 1991). Inclusion in buffers of sodium citrate to at least 25 mM blocks this interaction effectively, even at very high protein concentrations (e.g., 150 mg ml^{-1}). The mechanism responsible for this effect is not known, and no other tri- or tetracarboxylic acid compound that we tested was found to be effective. It is noteworthy that both the SO_4^{-2} ion (Wingfield *et al.*, 1991) and Chaps (which bears a sulfate group) have a strong solubilizing effect on Rev: it is also noteworthy that these two agents and citrate bear negative charges.

Rev filaments also engage in end-to-side interactions. These are less of a problem than the side-to-side interaction described above but are noticeable in electron micrographs of filaments (data not shown). This latter interaction can be suppressed by including 20 μg ml^{-1} protamine sulfate in the buffer, as attested both by electron microscopy and by a slight shift toward the included volume observed when filaments are subjected to size-exclusion chromatography in the presence of this additive. Poly-L-lysine, another polycation, however is not effective.

When Rev is folded and polymerized, the resulting filaments vary in length in a manner that depends on the initial protein concentration: at higher concentrations, more nucleation events occur, resulting in a shorter average length. When such short filaments are concentrated, either by pelleting or by ultrafiltration, much longer particles are recovered. Populations of quite uniform length may be obtained by stabilizing the filaments by cross-linking with 0.75 mM BS^3 to suppress dissociation and/or regrowth and then fractionating them according to size by gel filtration (see Materials and Methods). This procedure proved superior to the alternative method of ultrasonic fragmentation of long filaments.

Electron microscopic observations. Rev filaments formed at low protein concentrations are typically long, uniform, unbranched, and somewhat flexible. As visualized by negative staining with uranyl acetate (Fig. 2B), their outer diameter is ~15 nm, and they have an axial channel whose apparent width varies according to staining conditions, but is usually 5 to 7 nm. These images give no conspicuous indications of surface periodicities, but fine serrations are sometimes discernible along the edges. In an alternative protocol, filaments were examined in the STEM after negative staining with methylamine

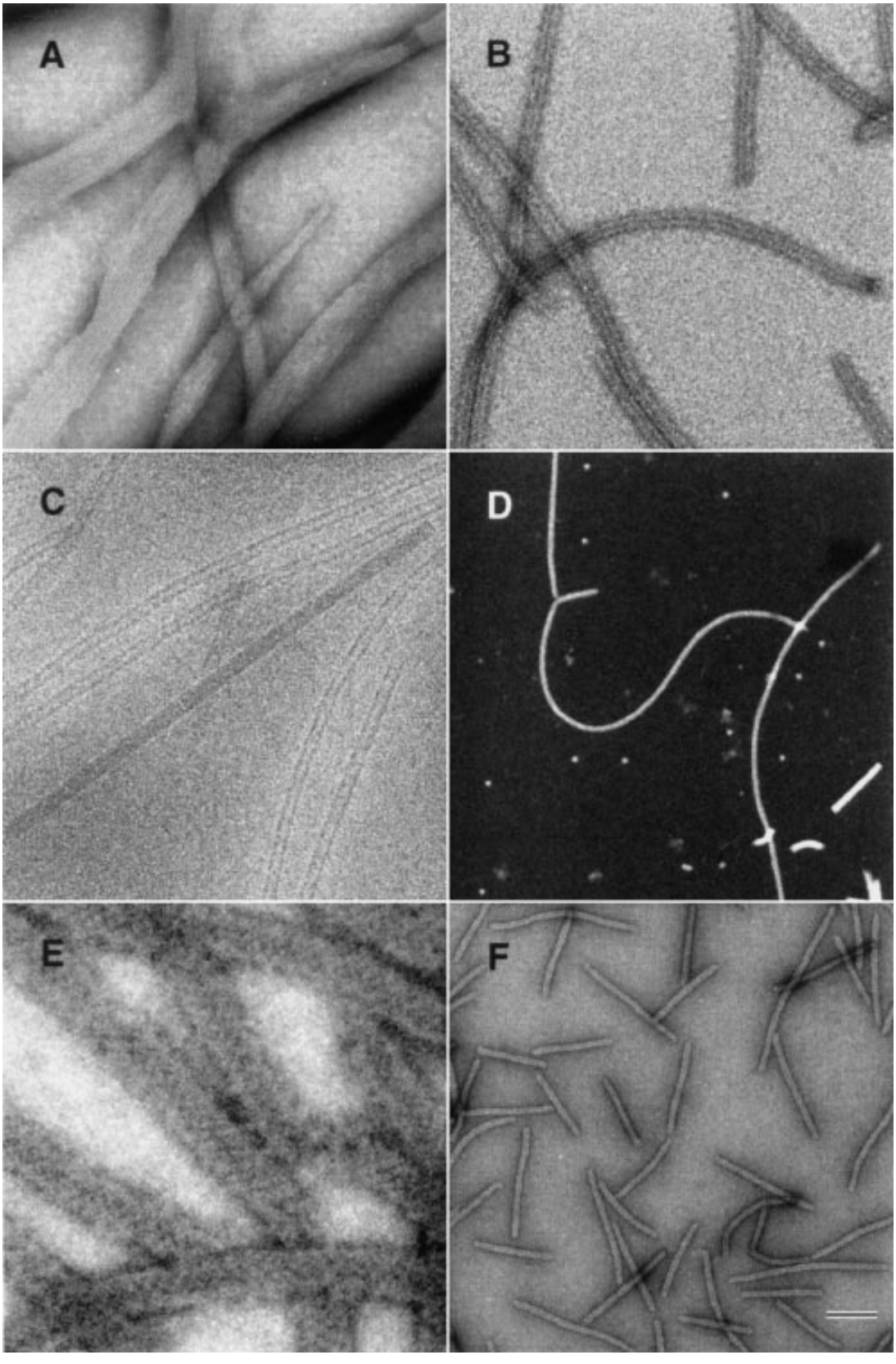

FIG. 2. (A) Rev filaments aggregated laterally in the absence of citrate. (B) Rev filaments negatively stained with 1% uranyl acetate. (C) Filaments visualized by cryo-electron microscopy. TMV particles have been added as an internal standard. (D) Filaments freeze-dried and visualized in the STEM. (E) Rev filaments stained with methylamine vanadate and observed in the STEM. (F) Shortened filaments formed at higher protein concentrations. Bar corresponds to 120 nm in A, D, and F; 60 nm in B and C; and 15 nm in E.

vanadate (Hainfeld *et al.*, 1994), and well contrasted specimens were found to exhibit marked cross-striations (Fig. 2E).

The linear density of the filaments was determined by dark-field STEM microscopy after preparation by freeze-drying (Fig. 2D). The resulting measurements observe a unimodal distribution that averages 69.6 ± 7.4 kDa nm^{-1} (SD, $n = 145$; Fig. 3).

The axial channel seen in negative staining was barely discernible in the freeze-dried specimens (cf. Figs. 2B and 2D), although the latter specimens give unambiguous definition of the outer edges. To clarify these features, axially averaged projections were calculated for both kinds of specimens and compared in Fig. 4 with a similar trace obtained from micrographs of frozen-hydrated specimens (e.g., Fig. 2C). With the latter specimens, which give superior preservation of native structure (Adrian *et al.*, 1984) the axial channel is again strongly represented in the transverse density profile (Fig. 4C), confirming the observation by negative staining. Filaments preserved in ice appear slightly straighter than in negative stain, although less so than nearby TMV particles. When confined to thin films, the filaments tend to pack laterally, though the long-range order is not high.

Determination of helical structure. Our intended strategy was the conventional approach of analyzing the layer-line structure of Fourier transforms of filament images after computational straightening, with the STEM mass-per-unit-length data providing an additional constraint. For this purpose, at least two layer lines are required (or two unambiguously indexed reflections on the same layer line). Despite considerable effort with negatively stained specimens, we only managed to resolve a single layer line at an axial spacing of ~$(5.3\ nm)^{-1}$. This layer line exhibits a single reflection with a pitch angle of ~45°, which correlates with the diagonal striations seen in STEM images of vanadate-stained filaments (see above). In one effort to enhance weak layer lines that may be present, we attempted to form "rafts" of parallel-packed filaments on lipid monolayers (Newman, 1991). Diffraction analysis of the resulting images (e.g., Fig. 5) demonstrated the $(5.1\ nm)^{-1}$ layer line strongly, but no additional reflections.

This problem was eventually solved by combining many diffraction patterns from individual filaments depicted in cryo-electron micrographs (Fig. 6A). The resulting composite pattern clearly contains a sec-

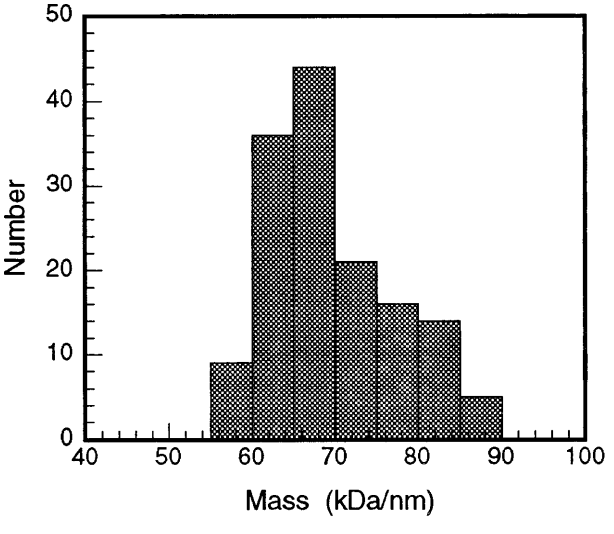

FIG. 3. Distribution of mass-per-unit-length measurements of freeze-dried Rev filaments as determined from STEM micrographs such as Fig. 1D. The mean density is 69.6 ± 7.4 kDa nm^{-1}.

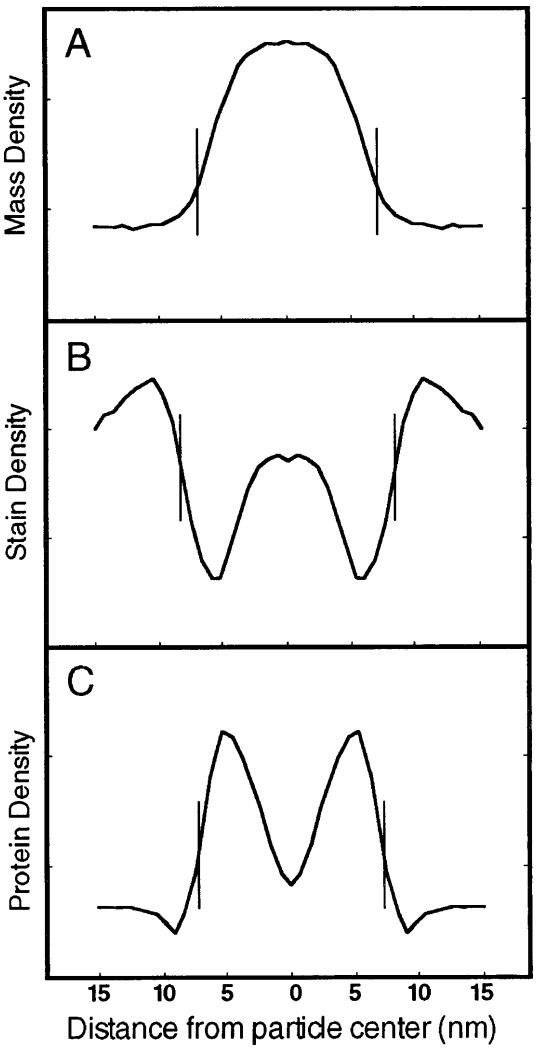

FIG. 4. Transverse density profiles of Rev filaments. The filaments were (A) freeze-dried, (B) negatively stained with uranyl acetate, and (C) frozen hydrated. The estimated diameters (indicated by the vertical bars) are 14.8, 17.2 ± 9, and 15.2 ± 5 nm in A through C, respectively. Density units are shown normalized.

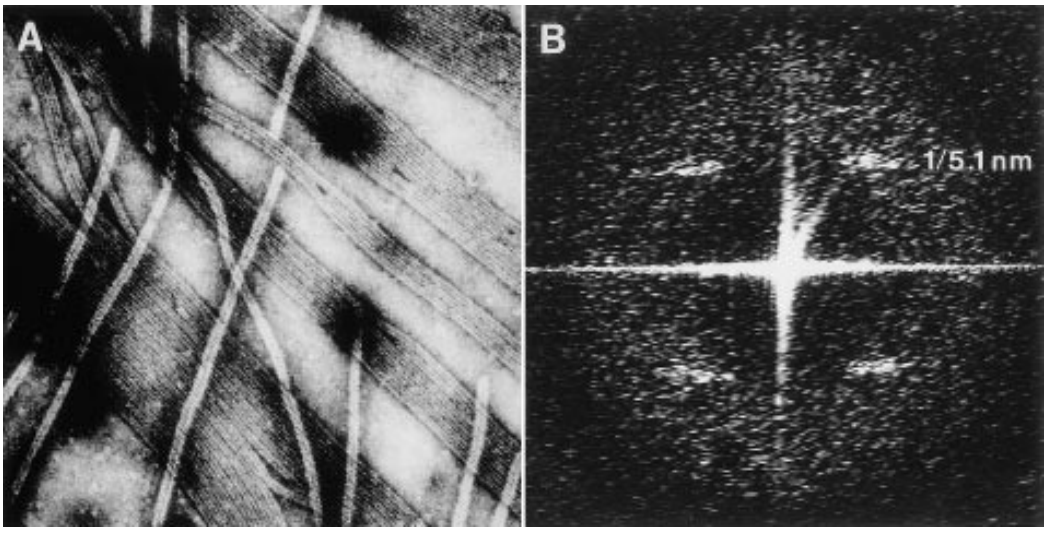

FIG. 5. (A) Negatively stained rafts of Rev filaments formed under lipid monolayers. (B) The corresponding optical diffraction pattern. One layer line at a spacing of $(5.1\ \text{nm})^{-1}$ is observed.

ond layer line at an axial spacing of $(3.4\ \text{nm})^{-1}$. Both layer lines were studied in detail in individual Fourier transforms in which the reflections could be seen to have significant intensity. Comparing the phases on either side of the meridian established that both reflections represent even-order Bessel functions. The radial coordinate of the reflections' intensity maxima, taken in conjunction with the filament radius (Materials and Methods), implied that the Bessel order was likely to be 6. The uncertainty arising from specifying the effective radius of the filament (Trus and Steven, 1984) is low in this case because the walls are so thin (see below). Taking into account the ratio of the axial spacings of the two layer lines, the requirement that an integral number of subunits should be associated with each lattice point, and the STEM mass-per-unit-length determination, a satisfactory solution was determined to be

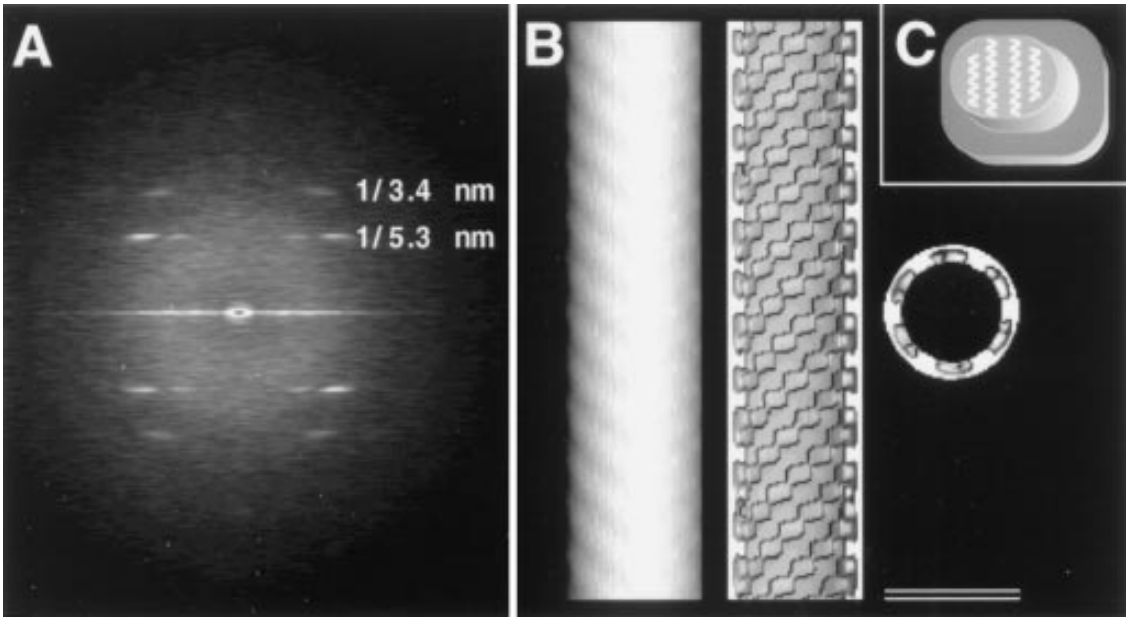

FIG. 6. (A) Averaged computed diffraction pattern of Rev filaments. The spacings of the two principal layer lines are indicated. The first zero of the contrast transfer function is apparent and occurs at $(2.1\ \text{nm})^{-1}$. (B) Surface-rendered density map of the Rev filaments at 2.1 nm resolution. Exterior, interior, and cross-sectional views are shown left to right. The hand is arbitrary. Each protrusion visible in the cut-away view corresponds to a molecular dimer of Rev. (C) A model of the morphological unit, composed of a Rev dimer as seen from inside the filament, showing the rim, central protrusion, and the proposed orientation of the helices. Bar, 15 nm.

a six-start helix of Rev dimers. The helical selection rule is given by

$$l = \pm 2n + 31m; n = 6n',$$

where l, n, m, and n' are integers, l corresponds to a layer line in the diffraction pattern, m is the number of subunits in n turns, and n' identifies the rotational symmetry of the structure (Misell, 1978). A density map was calculated, including data to a limit of $(2.1\ \text{nm})^{-1}$, which is close to the first zero of the contrast transfer function for these micrographs. The surface-rendered map (Fig. 6B) shows the six-start family of helices with their pitch angle of 45.3° and interstrand spacing of 3.8 nm. The filaments are smooth on the outside while the morphological units, corresponding to molecular dimers, protrude prominently on the inside. The filaments have an outer diameter of ~14.8 nm, in agreement with estimates based on transverse density profiles (Fig. 4). At this contour level—chosen to give plausible continuity of density and to enclose approximately the expected protein mass (actually, 120% of expected mass—see Conway *et al.*, 1996)—the protrusions are approximately 3.2 nm in diameter, and the walls are 2.2 nm thick. We have not been able to determine the handedness of the helices by metal shadowing, presumably because the outer surface of the filament is so smooth (Fig. 6B).

Secondary structure determination by Raman spectroscopy. Previously, circular dichroism has been used to estimate the α-helical content of purified Rev as ~48% (Wingfield *et al.*, 1991). We have now analyzed the secondary structure of polymerized Rev by Raman spectroscopy (Williams, 1986), a technique that is less susceptible to uncertainties caused by light scattering when applied to proteins in large aggregates. Analysis of the Raman spectrum (Fig. 7) yielded an α-helical content of 54% (Table I), very consistent with the estimate from CD. This concordance further shows that essentially no change in secondary structure takes place when Rev assembles into filaments. Moreover, the Raman spectrum suggests an approximate mutual alignment of these helices, in that the proteins of known structure in the database used in this calculation which Rev was found to resemble (i.e., which had high regression coefficients) have this property (Williams, 1986). These data are consistent with the helix-turn-helix motif proposed for the amino-terminal half of Rev (Fig. 1; Auer *et al.* 1994; Thomas *et al.*, 1997).

X-ray fiber diffraction. Fiber diffraction has been used to solve several filamentous particles, including TMV to 0.29 nm resolution (Namba *et al.*, 1989). Noting that Rev has a number of properties in common with TMV coat protein (Wingfield *et al.*, 1991), we sought to apply this method. To improve

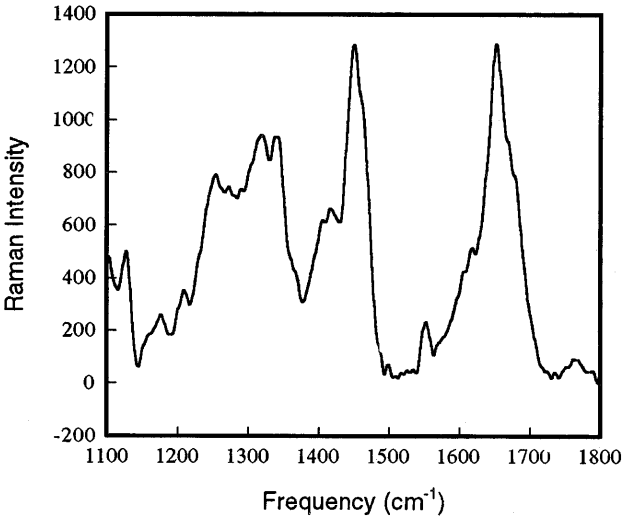

FIG. 7. Raman spectrum of Rev filaments at 20°C. The amide III region (1220 to 1340 cm^{-1}) and the amide I region (1620 to 1720 cm^{-1}) are characteristic of a protein with both a high fraction of alpha helix and significant antiparallel beta sheet. Amide bands characteristic of helix are seen at 1320 and 1653 cm^{-1}. The amide bands due to beta sheet are seen at 1254 cm^{-1} and a shoulder at 1670 cm^{-1}.

the prospects of obtaining well-ordered fibers, filaments of approximately uniform length were prepared (see above). Particles with an aspect ratio of ~18 were chosen because both theoretical considerations and practical experience indicate that they are optimal for alignment (I. Yamashita and K. Namba, personal communication). As monitored by polarizing microscopy (Fig. 8), concentrated suspensions of these particles readily formed tactoids which could be aligned, either by drying into fibers between opposed glass rods or, more effectively, by laminar flow-induced shear in quartz capillaries to form liquid crystals (Gregory and Holmes, 1965). However, these specimens did not yield any detectable reflections in the X-ray beam, presumably due to disorder in the liquid crystal not detectable at the

TABLE I

Secondary Structure Content of Filamentous Rev from Raman Spectra

	Amide I			Amide III		
Structure	Helix	Beta	Turn	Helix	Beta	Turn
Content[a]	53 ± 4	20 ± 3	11 ± 2	54 ± 5	24 ± 6	12 ± 5

Note. The sum of structure contents was 94.4% in the amide I analysis and 100% in the amide III analysis. Unidentified structure content, the remainder from 100%, is not shown. Standard deviations represent differences between Raman and X-ray diffraction measurements for the reference.

[a] Percent structure and standard deviation.

light microscope level (G. Stubbs, personal communication).

Electron diffraction. Electron microdiffraction of aligned Rev filaments was undertaken with a view of determining the orientation of the α-helices relative to the filament axis. For these experiments, concentrated preparations of filaments were smeared onto thin carbon films and quenched in liquid ethane. At least partial alignment of the filaments was achieved (Fig. 9). Electron diffraction produced a meridional arc with a spacing of approximately $(0.51\ nm)^{-1}$ (Fig. 9, inset), indicative of α-helices (Wilson, 1966). The meridional setting of this reflection suggests that the α-helices are in approximate alignment with the long axis of the filament.

Attempts were made to form larger and more regular arrays, to improve the electron diffraction patterns. Formation of arrays, from either preformed or *de novo* polymerized filaments, on monolayers prepared from a variety of charged and neutral lipids met with only limited success (see above and Fig. 5). Similarly, Rev filaments formed only small arrays by either flow alignment or spreading on mica (Ruiz *et al.*, 1994). Rev filaments mixed with small amounts (0.5%) of high-molecular-weight poly(acrylamide-coacrylic acid) (15 MDa) were readily drawn into fibers 60 to 100 nm in diameter, but did not yield ordered diffraction.

FIG. 8. Alignment of Rev filaments for fiber X-ray diffraction. (A) Rev filaments with an aspect ratio of about 18 and at a concentration of 150 mg ml^{-1} in HSSE as initially drawn into a 0.2-mm-i.d. capillary. (B) Columnar phase obtained by shear alignment of A. The meniscus and some unaligned material are visible at the top. Capillaries were photographed between crossed polarizers at an angle of 45°.

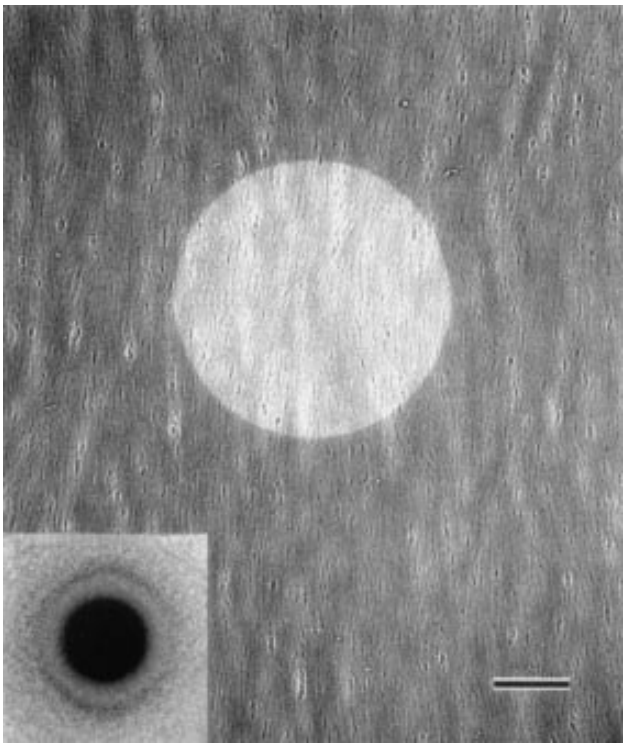

FIG. 9. Electron diffraction of Rev filaments. A cryo-electron micrograph of aligned Rev filaments. The circular area was selected to record the electron diffraction pattern. (Inset) The corresponding electron diffraction pattern with a broad $(5.1\ Å)^{-1}$ reflection. The diffraction pattern was computationally filtered to reduce the background due to inelastically scattered electrons. Bar, $(5.0\ Å)^{-1}$ in the diffraction pattern and 750 nm in the micrograph.

Structure of the filament and the Rev dimer. Approximately half of the mass of each morphological unit resides in the protrusion that extends from the thin flat outer shell toward the filament axis. Thus, the Rev dimer has the overall shape of a top-hat with a slightly squared cylinder. The disposition of the two monomers within the Rev dimer cannot be discerned at the resolution of our current reconstruction (2.1 nm). However, the spectroscopic data reveal that approximately half of each Rev subunit is α-helical, and earlier analyses imply that the α-helices are found mainly in the amino half of the protein (see Fig. 1). Both our Raman data and previous sequence analyses (Thomas *et al.*, 1997; Auer *et al.* 1994) suggest an aligned arrangement of the helices within the monomer. The electron diffraction results in turn indicate that the helices are predominantly oriented in alignment with the filament axis. To within the limits of the resolution of this reconstruction the dimensions of the protrusions in this direction (~2.6 nm) are compatible with the predicted mean lengths of the helices (~2.7 nm).

The nature of the thin areas of the wall is uncer-

tain. Raman spectroscopy indicates that Rev contains ~24% antiparallel beta sheet. If we assume that this fold is essentially restricted to the carboxy-terminal half of the protein, up to 50% of the outer wall may be composed of antiparallel beta sheet. In keeping with this, the DSC neural net secondary structure prediction (King and Sternberg, 1996) shows three distinct regions of beta sheet within the carboxy-terminal half of the protein (Fig. 1). The thinnest areas of the wall measure approximately 0.6 nm, at the current contour level, in good agreement with the 0.7-nm thickness typical of beta sheets.

Regulation of filament assembly. The question arises, how does Rev assemble into filaments? At very low concentrations, Rev probably exists as a monomer (Cole *et al.*, 1993) or possibly as a dimer (Wingfield *et al.*, 1991), while at somewhat higher concentrations gel filtration (Nalin *et al.*, 1990) and chemical cross-linking (Zapp *et al.*, 1991) indicate a tetramer. Above the critical concentration of 80 μg ml^{-1}, Rev assembles into filaments (Wingfield *et al.*, 1991). In the case of assembly onto the RRE it is probable that only a monomer binds to the high-affinity site (Zemmel *et al.*, 1996; Iwai *et al.*, 1992). Our structural analysis indicates that the hollow filaments formed in the absence of RNA are assembled from dimers. For comparison, other nucleic acid binding proteins with a helix-turn-helix motif and an adjacent beta sheet domain, such as HU (Vis *et al.*, 1994), also dimerize.

Finally, how the filaments studied here relate to those formed in the presence of cognate RNA is not clear. However, they may have some functional significance. Rev has been shown to function as a nucleocytoplasmic shuttle protein (Görlich and Mattaj, 1996; Fritz and Green, 1996; Gerace, 1995). Kubota *et al.* (1992) have shown that a nonfunctional mutant of Rev (dRev) with a deletion in the nuclear localization signal not only accumulated in the cytoplasm but also inhibited the nuclear import of coexpressed wild-type Rev. The authors concluded that dRev inhibited Rev function by heterooligomerization and, consequently, that Rev multimerizes in the cytoplasm before import into the nucleus. A similar conclusion was recently reached by Szilvay *et al.* (1997). The *in vitro* formed filaments described here may, though they are artificially long, be representative of the multimerized form of the protein that accumulates *in vivo* prior to (re)import into the nucleus.

SUMMARY

We have determined the structure of Rev filaments formed in the absence of RNA. These filaments may be related to the form in which Rev accumulates at the nuclear envelope prior to import. They consist of a six-start set of helices of molecular dimers, with 31 subunits in two turns. Taking into account spectroscopic and other data, a tentative model is proposed, wherein the α-helices in the amino-terminal domain of Rev are in approximate alignment with each other and with the filament axis and are probably located on the inner surface of the filament wall. The carboxy-terminal domain, putatively composed in part of antiparallel beta sheet, may form the smooth outer surface.

The authors thank Drs. Martha Simon and James Hainfeld at the Brookhaven National Laboratory for provision of STEM micrographs, Drs. Frank Booy and Henri Chanzy (CERMAV-CNRS, Grenoble, France, on sabbatical leave at the National Institutes of Standards and Technology, Gaithersburg, MD) for kindly performing the cryo-electron diffraction experiments, Dr. Gerald Stubbs at Vanderbilt University for performing the X-ray fiber diffraction experiments, Joshua Kaufman and Ira Palmer of the NIH Protein Expression Laboratory for expert technical assistance, Dr. James Conway for provision of computing facilities, and Dr. Michal Jarnik for assistance with electron microscopy.

REFERENCES

Adrian, M., Dubochet, J., Lepault, J., and McDowall, A. W. (1984). Cryo-electron microscopy of viruses, *Nature* **308,** 32–36.

Antoni, B. A., Stein, S., and Rabson, A. B. (1994). Regulation of human immunodeficiency virus infection: Implications for pathogenesis, *Adv. Virus Res.* **43,** 53–145.

Arrigo, S., and Chen, I. S. Y. (1991). Rev is necessary for translation but not cytoplasmic accumulation of HIV-1 vif, vpr, and env/vpu 2 RNAs, *Genes Dev.* **5,** 808–819.

Auer, M., Gremlich, H.-U., Seifert, J.-M., Daly, T. J., Parslow, T. G., Casari, G., and Gstach, H. (1994). Helix-loop-helix motif in HIV-1 Rev, *Biochemistry* **33,** 2988–2996.

Battiste, J. L., Hongyuan, M., Rao, N. S., Tan, R., Muhandiram, D. R., Kay, L. E., Frankel, A. D., and Williamson, J. R. (1996). α-helix-RNA major groove recognition in an HIV-1 Rev peptide-RRE RNA complex, *Science* **273,** 1547–1551.

Bevec, D., Jaksche, H., Oft, M., Wöhl, T., Himmelspach, M., Pacher, A., Schebesta, M., Koettnitz, K., Dobrovnik, M., Csonga, R., Lottspeich, F., and Hauber, J. (1996). Inhibition of replication in lymphocytes by mutants of the Rev cofactor eIF-5A, *Science* **271,** 1858–1860.

Bogerd, H. P., Fridell, R. A., Madore, S., and Cullen, B. R. (1995). Identification of a novel cellular co-factor for the Rev/Rex class of retroviral proteins, *Cell* **82,** 485–494.

Booy, F. P., Newcomb, W. W., Trus, B. L., Brown, J. C., Baker, T. S., and Steven, A. C. (1991). Liquid-crystalline phage-like packing of encapsidated DNA in Herpes simplex virus, *Cell* **64,** 1007–1015.

Cole, J. L., Gehman, J. D., Shafer, J. A., and Kuo, L. C. (1993). Solution oligomerization of the Rev protein of HIV-1: Implications for function, *Biochemistry* **32,** 11769–11775.

Conway, J. F., Trus, B. L., Booy, F. P., Newcomb, W. W., Brown, J. C., and Steven, A. C. (1996). Visualization of three-dimensional density maps reconstructed from cryoelectron micrographs of viral capsids, *J. Struct. Biol.* **116,** 200–208.

Cullen, B. R. (1992). Mechanism of action of regulatory proteins encoded by complex retroviruses, *Microbiol. Rev.* **56,** 375–394.

Daly, T. J., Doten, R. C., Rennert, P., Auer, M., Jaksche, H.,

Donner, A., Fisk, G., and Rusche, J. R. (1993). Biochemical characterization of binding of multiple HIV-1 Rev monomeric proteins to the Rev response element, *Biochemistry* **32,** 10497–10505.

Fisher, U., Meyer, S., Teufel, M., Heckel, C., Lührman, R., and Rautmann, G. (1994). Evidence that HIV-1 Rev directly promotes the nuclear export of unspliced RNA, *EMBO J.* **13,** 4105–4112.

Fisher, U., Huber, J., Boelens, W. C., Mattaj, I. W., and Lührman, R. (1995). The HIV-1 Rev activation domain is a nuclear export signal that accesses an export pathway used by specific cellular RNAs, *Cell* **82,** 475–483.

Fritz, C. C., and Green, M. R. (1996). HIV Rev uses a conserved cellular protein export pathway for the nucleocytoplasmic transport of viral RNAs, *Curr. Biol.* **6,** 848–854.

Gerace, L. (1995). Nuclear export signals and the fast track to the cytoplasm, *Cell* **82,** 341–344.

Görlich, D., and Mattaj, I. W. (1996). Nucleocytoplasmic transport, *Science* **271,** 1513–1518.

Gregory, J., and Holmes, K. (1965). Methods of preparing oriented tobacco mosaic virus sols for X-ray diffraction, *J. Mol. Biol.* **13,** 796–801.

Hainfeld, J. F., Safer, D., Wall, J. S., Simon, M., Li, B., and Powell, R. D. (1994). *in* Bailey, G. W., and Garrat-Reed, A. J. (Eds.), Proceedings of the 52nd Annual Meeting of the Micros. Society of America, pp. 132–133, San Francisco.

Heaphy, S., Finch, J. T., Gait, M. J., Karn, J., and Singh, M. (1991). Human immunodeficiency virus type 1 regulator of virion expression, Rev, forms nucleo-protein filaments after binding to a purine-rich "bubble" located within the rev-response region of viral RNA, *Proc. Natl. Acad. Sci. USA* **88,** 7366–7370.

Heck, D. V., Trus, B. L., and Steven, A. C. (1996). Three-dimensional structure of *Bordetella pertussis* fimbriae, *J. Struct. Biol.* **116,** 264–269.

Iwai, S., Pritchard, C., Mann, D. A., Karn. J., and Gait, M. J. (1992). Recognition of the high affinity site in rev-response element RNA by the human immunodeficiency virus type-1 rev protein, *Nucleic Acids Res.* **20,** 6465–6472.

Jain, C., and Belasco, J. G. (1996). A structural model for the HIV-1 Rev-RRE complex deduced from altered-specificity rev variants isolated by a rapid genetic strategy, *Cell* **87,** 115–125.

Karn, J., Dingwall, C., Gait, M. J., Heaphy, S., and Skinner, M. A. (1991). *in* Eckstein, F., and Lilley, D. M. J. (Eds.), Nucleic Acids and Molecular Biology, Vol. 5, pp. 194–218, Springer-Verlag, Berlin.

Kim, N.-H., Herth, W., Vuong, R., and Chanzy, H. (1996). The cellulose system in the cell wall of *Micrasterias*, *J. Struct. Biol.* **117,** 195–203.

King, R. D., and Sternberg, M. J. (1996). Identification and application of the concepts important for accurate and reliable protein secondary structure prediction, *Protein Sci.* **5,** 2298–2310.

Kingsman, S. M., and Kingsman, A. J. (1996). The regulation of human immunodeficiency virus type-1 gene expression, *Eur. J. Biochem.* **240,** 491–507.

Kjems, J., Frankel, A. D., and Sharp, P. A. (1993). Specific regulation of mRNA splicing *in vitro* by a peptide from HIV-1 Rev, *Cell* **67,** 169–178.

Kubota, S., Furuta, R., Maki, M., and Hatanaka, M. (1992). Inhibition of human immunodeficiency virus type 1 rev function by a rev mutant which interferes with nuclear/nucleolar localization of rev, *J. Virol.* **66,** 2510–2513.

Lawrence, J., Cochrane, A., Johnson, C. V., Perkins, A., and Rosen, C. A. (1991). The HIV-1 Rev protein: A model system for coupled RNA transport and translation, *New Biol.* **3,** 1220–1232.

Levy, J. A. (1993). Pathogenesis of human immunodeficiency virus, *Microbiol. Rev.* **57,** 183–289.

Malim, M. H., and Cullen, B. R. (1991). HIV-1 structural gene expression requires the binding of multiple Rev monomers to the viral RRE: Implications for HIV-1 latency, *Cell* **65,** 241–248.

Misell, D. L. (1978). *in* Glauert, A. M. (Ed.), Practical Methods in Electron Microscopy, Vol. 7, North-Holland, Amsterdam.

Nalin, C. M., Purcell, R. D., Antelman, D., Meuller, D., Tomchak, L., Wegrzynski, B., McCarney, E., Toome, V., Kramer, R., and Hsu, H.-C. (1990). Purification and characterization of recombinant Rev protein of human immunodeficiency virus type-1, *Proc. Natl. Acad. Sci. USA* **87,** 7593–7597.

Namba, K., Pattanayek, R., and Stubbs, G. (1989). Visualization of protein–nucleic acid interactions in a virus. Refined structure of intact tobacco mosaic virus at 2.9 Å resolution by X-ray fiber diffraction, *J. Mol. Biol.* **208,** 307–325.

Newman, R. H. (1991). Two-dimensional crystallization of proteins on lipid monolayers, *Electron Microsc. Rev.* **14,** 197–203.

Rosen, C. A., and Fenyoe, E. M. (1995). Virology, an overview, *AIDS* **9,** S1–S3.

Ruiz, T., Ranck, J.-L., Diaz-Avalos, R., Caspar, D. L. D., and DeRosier, D. J. (1994). Electron diffraction of helical particles, *Ultramicroscopy* **55,** 383–395.

Steven, A. C., Stall, R., Steinert, P. M., and Trus, B. L. (1986). *in* Metuzals, J. (Ed.), Electron Microscopy and Alzheimer's Disease, pp. 31–33, San Francisco Press, San Francisco.

Stutz, F., Neville, M., and Rosbash, M. (1995). Identification of a novel nuclear pore-associated protein as a functional target of the HIV-1 Rev protein in yeast, *Cell* **82,** 495–506.

Szilvay, A. M., Brokstad, K. A., Bøe, S.-O., Haukenes, G., and Kalland, K.-H. (1997). Oligomerization of HIV-1 Rev mutants in the cytoplasm and during nuclear import, *Virology* **235,** 73–81.

Thomas, D., Schultz, P., Steven, A. C., and Wall, J. S. (1994). Mass analysis of biological macromolecular complexes by STEM, *Biol. Cell.* **80,** 181–192.

Thomas, S., Hauber, J., and Casari, G. (1997). Probing the structure of the HIV-1 transactivator protein by functional analysis, *Protein Eng.* **10,** 103–107.

Torbet, J. (1987). Using magnetic orientation to study structure and assembly, *Trends Biochem. Sci.* **12,** 327–330.

Trus, B. L., Kocsis, E., Conway, J. F., and Steven, A. C. (1996). Digital image processing of electron micrographs: The PIC system-III, *J. Struct. Biol.* **116,** 61–67.

Trus, B. L., and Steven, A. C. (1984). Diffraction patterns from stained and unstained helices: Consistency or contradiction? *Ultramicroscopy* **15**, 325–335.

Vis, H., Boelens, R., Mariani, M., Stroop, R., Vorgias, C. E., Wilson, K. S., and Kaptein, R. (1994). ^{1}H, ^{13}C, and ^{15}N resonance assignments and secondary structure analysis of the HU protein from *Bacillus stearothermophilus* using two- and three-dimensional double- and triple-resonance heteronuclear magnetic resonance spectroscopy, *Biochemistry* **33,** 14858–14870.

Wall, J. S., and Hainfeld, J. F. (1986). Mass mapping with the scanning transmission electron microscope, *Annu. Rev. Biophys. Chem.* **15,** 355–376.

Wang, H., and Stubbs, G. (1994). Structure determination of cucumber green mottle mosaic virus by X-ray fiber diffraction. Significance for the evolution of tobamoviruses, *J. Mol. Biol.* **239,** 371–384.

Williams, R. W. (1986). Protein secondary structure analysis using Raman amide I and amide III spectra, *Methods Enzymol.* **130,** 311–331.

Wilson, H. R. (1966). Diffraction of X-rays, Edward Arnold, London.

Wingfield, P. T., Stahl, S. J., Payton, M. A., Venkatesan, S., Misra, M., and Steven, A. C. (1991). HIV-1 Rev expressed in recombinant *Escherichia coli*: Purification, polymerization, and conformational properties. *Biochemistry* **30,** 7527–7534.

Zapp, M. L., Hope, T. J., Parslow, T. G., and Green, M. R. (1991). Oligomerization and RNA binding domains of the type 1 human immunodeficiency virus Rev protein: A dual function for an arginine-rich binding motif, *Proc. Natl. Acad. Sci. USA* **88,** 7734–7738.

Zemmel, R. W., Kelley, A. C., Karn, J., and Butler, P. J. G. (1996). Flexible regions of RNA structure facilitate co-operative Rev assembly on the Rev-response element, *J. Mol. Biol.* **258,** 763–777.